# Ultrafast spin tunneling and injection in coupled nanostructures of InGaAs quantum dots and quantum well

Xiao-Jie Yang, Takayuki Kiba, Takafumi Yamamura, Junichi Takayama, Agus Subagyo, Kazuhisa Sueoka, and Akihiro Murayama

Citation: Applied Physics Letters **104**, 012406 (2014); doi: 10.1063/1.4861387
View online: http://dx.doi.org/10.1063/1.4861387
View Table of Contents: http://scitation.aip.org/content/aip/journal/apl/104/1?ver=pdfcov
Published by the AIP Publishing

# Ultrafast spin tunneling and injection in coupled nanostructures of InGaAs quantum dots and quantum well

Xiao-Jie Yang,[a] Takayuki Kiba, Takafumi Yamamura, Junichi Takayama, Agus Subagyo, Kazuhisa Sueoka, and Akihiro Murayama[b]
*Graduate School of Information Science and Technology, Hokkaido University, Kita 14, Nishi 9, Kita-ku, Sapporo 060-0814, Japan*

(Received 9 October 2013; accepted 20 December 2013; published online 9 January 2014)

We investigate the electron-spin injection dynamics via tunneling from an $In_{0.1}Ga_{0.9}As$ quantum well (QW) to $In_{0.5}Ga_{0.5}As$ quantum dots (QDs) in coupled QW-QDs nanostructures. These coupled nanostructures demonstrate ultrafast (5 to 20 ps) spin injection into the QDs. The degree of spin polarization up to 45% is obtained in the QDs after the injection, essentially depending on the injection time. The spin injection and conservation are enhanced with thinner barriers due to the stronger electronic coupling between the QW and QDs. © *2014 AIP Publishing LLC*. [http://dx.doi.org/10.1063/1.4861387]

Strong three-dimensional quantum confinement results in atom-like discrete energy levels and significantly suppresses carrier- or exciton- spin relaxation in self-assembled semiconductor quantum dots (QDs).[1,2] Therefore, semiconductor QDs provide excellent platforms for initializing, manipulating, and probing the spin states of electron, hole or exciton,[3–7] and realization of spin-functional photonic devices.[8–12] Efficient spin injection, namely, the spatial transfer of spin-polarized carriers or excitons into QDs, is prerequisite for these applications. For this subject, the spin-injection from an adjacent 2-dimensional electronic system of InGaAs quantum well (QW) into QDs has three advantages: First, more than 50% initial spin polarization of excitons can be obtained in the QW due to the lifted degeneration of hole bands;[9] Second, ultrafast spin injection from the QW into QDs via spin-conserved tunneling is possible;[13–15] Last, the spin relaxation is suppressed because the small energy difference between the initial state in the QW and the final states in the QDs. In this letter, we study the optical spin-injection dynamics as a function of the thickness of the tunneling barrier in the coupled nanostructures of $In_{0.5}Ga_{0.5}As$ QDs with an $In_{0.1}Ga_{0.9}As$ QW.

The coupled QW-QDs samples were grown by molecular beam epitaxy. A 400-nm-thick GaAs buffer layer was grown on a (001) GaAs substrate at 580 °C. Then, a 20-nm-$In_{0.1}Ga_{0.9}As$ QW and GaAs barrier were grown at 520 °C. The barrier thickness, $d$, was varied from 2 to 20 nm. The substrate temperature was subsequently decreased to 480 °C for the self-assembled growth of an $In_{0.5}Ga_{0.5}As$-QD layer with a nominal thickness of 1.8 nm. Finally, the QD-layer was capped by a 50-nm-thick GaAs layer at an elevated temperature from 480 °C to 580 °C. An image of high-angle annular dark field (HAADF) scanning transmission electron microscopy (STEM) (see Fig. 1(a)) clearly shows the single-crystal epitaxial nanostructure of lens-shaped $In_{0.5}Ga_{0.5}As$ QDs with diameter and height of 20 nm and 3.5 nm, respectively, 6-nm-thick GaAs barrier and 20-nm-thick $In_{0.1}Ga_{0.9}As$ QW.

We performed transient optical spin-injection and -detection with time-resolved PL (TRPL) spectra simultaneously from both the QW and QDs. A mode-locked Ti:Sapphire laser with a wavelength of 840 nm, pulse width of 150 fs, and repetition frequency of 76 MHz, combined with a quarter-wave plate, was used for circularly polarized and selective excitation to the QW. An effect of a spectral tail of laser light was removed by using a sharp-cut filter. The TRPL spectra were measured at 20 K using a streak camera combined with a spectrometer, where the circularly polarized lights are discriminated by combining a quarter-wave plate with a linear polarizer. The time resolution was 5 ps, aided by a convolution calculation taking the time response of the measurement system into account.

Spin-independent carrier or exciton tunneling between a QW and QDs was recently discussed.[16–20] Similarly, if we consider the transfer of a spin-polarized electron as depicted in Fig. 1(b), its dynamics can be observed in TRPL from the QDs under resonant excitation to the QW with circularly polarized light pulses. We calculated the energy levels and wavefunctions of the carriers in the coupled nanostructures with various barrier thicknesses, by taking the 3-dimensional shape, size or thickness, composition, and the resultant strain into account. The ground state (GS)-wavefunction of an electron ($\psi^{e}_{QW}$, blue line) in the QW markedly penetrates into the QD, as shown in Fig. 1(b). The energy of this coupled state ($\psi^{e}_{QW}$) is slightly higher (about 30–60 meV) than that of the excited state (ES) ($\psi^{e}_{QD-ES}$) in the QD. Thus, the electron can spatially transfer from the QW onto the ES in the QD via tunneling and subsequent energy relaxation, rapidly emitting one longitudinal optical (LO) phonon and coupling with a few of acoustic phonons.[21,22] In contrast, a heavy hole (hh) wavefunction does not penetrate significantly. However, there are many excited states of the hh and light hole between the GS state in the QD part and the excitation energy. These hole states can act as an efficient channel of the hole injection. Then, an exciton state can be stabilized within the QD. We are primarily concerned with the spin-tunneling dynamics. By observing the transient spin states at the coupled GS, we can obtain information about the spin tunneling. Therefore, we observe circularly polarized TRPL

[a]Electronic mail: yangxj@ist.hokudai.ac.jp
[b]Electronic mail: murayama@ist.hokudai.ac.jp

 

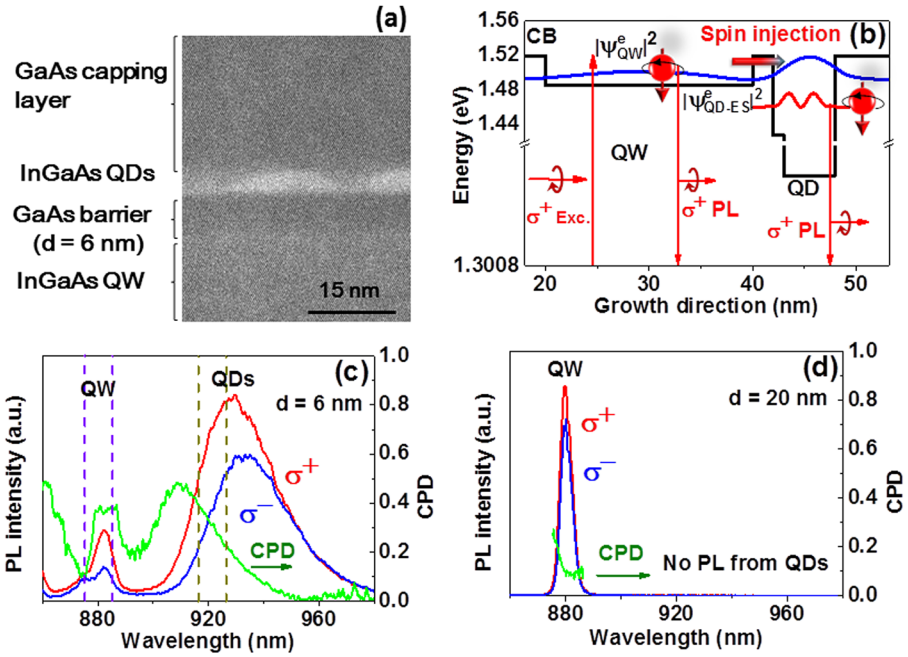


FIG. 1. (a) HAADF-STEM image of the coupled InGaAs QW-QDs nanostructure designed with a 6-nm-thick GaAs barrier. (b) Schematic drawing of electron-spin injection via tunneling in coupled InGaAs QW-QDs nanostructure with thin GaAs barrier. $\sigma^+$- (red lines) and $\sigma^-$- (blue lines) polarized PL spectra at 20 K and the corresponding CPD (green lines) for the coupled nanostructures with (c) $d = 6$ nm and (d) $d = 20$ nm, respectively. The broken lines in (c) indicate the wavelength regions for TRPL measurements in Figs. 2(c) and 2(d).

in the ESs in the QDs to directly get insight into the exciton-spin states resulting from the spin tunneling and governed by the optical rule. The spin relaxation, caused by the phonon-assisted energy relaxation, can be sufficiently suppressed because of the limited number of phonons involved in the energy relaxation. Figs. 1(c) and 1(d) show circularly polarized PL spectra and the corresponding circular polarization degree (CPD) for coupled QD samples with $d = 6$ and 20 nm, under $\sigma^+$-polarized quasi-resonant excitation with the energy slightly above the GS in the QW. Here, the CPD is defined as $(I_{\sigma+} - I_{\sigma-})/(I_{\sigma+} + I_{\sigma-})$, where $I_{\sigma^+}$ and $I_{\sigma^-}$ are the intensities of the $\sigma^+$- or $\sigma^-$-polarized PL. The former sample ($d = 6$ nm in Fig. 1(c)) displays strong $\sigma^+$-polarized (co-circular to the excitation polarization) PL spectra in the range from 900 nm to 960 nm, corresponding to the emissions from the ES in the QDs. The weaker PL peak at 882 nm originates from the GS state in the QW. In contrast, the latter sample ($d = 20$ nm in Fig. 1(d)) exhibits a significantly stronger but weakly $\sigma^+$-polarized PL peak only at 880 nm from the QW. The changes of these PL intensities with increasing barrier thickness imply that the electrons generated in the QW are transferred into the QDs in the former sample and such a transfer is strongly suppressed in the latter sample because of a sufficiently thick barrier against that from the QW. The direct generation of excitons in the QDs is negligible because of significantly weaker PL in the QD in Fig. 1(d). The generation of excitons in a wetting layer is also negligible, which is supported by an energy calculation of the wetting layer, where the lowest energy level in the wetting layer is above the GS in the QW. The appearance of the PL-CPD in the QDs in Fig. 1(c) indicates injection of spin-polarized excitons from the QW into QDs. The spin-polarized electrons can be injected rapidly via one LO-phonon emission from the ground state at the QW side into the excited states of the QDs before significant spin relaxation. The spin injection into lower-lying energy states in the QDs is affected by the spin-dependent filling effect[23,24] and acoustic-phonon assisted energy relaxation. As a result, the maximum peak of the CPD can appear at the energy close to about one-LO-phonon energy lower from the GS of the QW side.

The TRPL spectra recorded simultaneously from both the QW and QDs can provide direct information about the spin-injection dynamics. We establish a rate-equation model suitable for the present coupled QW-QD system. In this model, we assume that spin-polarized excitons generated in the QW transfer into the ES in the QD with an injection time of $\tau_{\text{inj}}$. The rate equations can be written as follow:

$$\frac{dN_0^{\sigma+}}{dt} = -\frac{N_0^{\sigma+}}{\tau_0}\left\{\eta_0^+\left(1-\frac{N_{\text{QW}}^{\sigma+}}{D_{\text{QW}}^{\sigma+}}\right)+\eta_0^-\left(1-\frac{N_{\text{QW}}^{\sigma-}}{D_{\text{QW}}^{\sigma-}}\right)\right\}, \quad (1)$$

$$\frac{dN_{\text{QW}}^{\sigma\pm}}{dt} = \frac{N_0^{\sigma+}}{\tau_0}\eta_0^{\pm}\left(1-\frac{N_{\text{QW}}^{\sigma\pm}}{D_{\text{QW}}^{\sigma\pm}}\right) - \left\{\frac{1}{\tau_{\text{QW}}^r}+\frac{1}{\tau_{\text{QW}}^{nr}}+\frac{1}{\tau_{\text{QW}}^{sr}}+\frac{1}{\tau_{inj}}\left(1-\frac{N_{\text{QD-ES}}^{\sigma\pm}}{D_{\text{QD-ES}}^{\sigma\pm}}\right)\right\}N_{\text{QW}}^{\sigma\pm} + \frac{N_{\text{QW}}^{\sigma\mp}}{\tau_{\text{QW}}^{sr}}, \quad (2)$$

$$\frac{dN_{\text{QD-ES}}^{\sigma\pm}}{dt} = \eta^{\pm}\left(1-\frac{N_{\text{QD-ES}}^{\sigma\pm}}{D_{\text{QD-ES}}^{\sigma\pm}}\right)\frac{N_{\text{QW}}^{\sigma\pm}}{\tau_{inj}} - \left(\frac{1}{\tau_{\text{QD-ES}}^r}+\frac{1}{\tau_{\text{QD-ES}}^{nr}}\right)N_{\text{QD-ES}}^{\sigma\pm} + \frac{N_{\text{QD-ES}}^{\sigma\mp}}{\tau_{\text{QD-ES}}^{sr}}, \quad (3)$$

where $N_0^{\sigma+}$ and $\tau_0$ represent an initial population of $\sigma^+$-polarized exciton and a relaxation time to the GS in the QW. The time-dependent populations at the GS level in the QW and the emissive ES levels in the QD, optically active with $\sigma^\pm$-polarizations, are $N_{\text{QW}}^{\sigma\pm}$ and $N_{\text{QD-ES}}^{\sigma\pm}$, respectively. Here, $\eta$ is a spin-conservation factor,[15] where $\eta = 1$ expresses full conservation of the spin state during relaxation or injection, while $\eta = 0.5$ expresses full relaxation, and $\eta^+ + \eta^- = 1$.

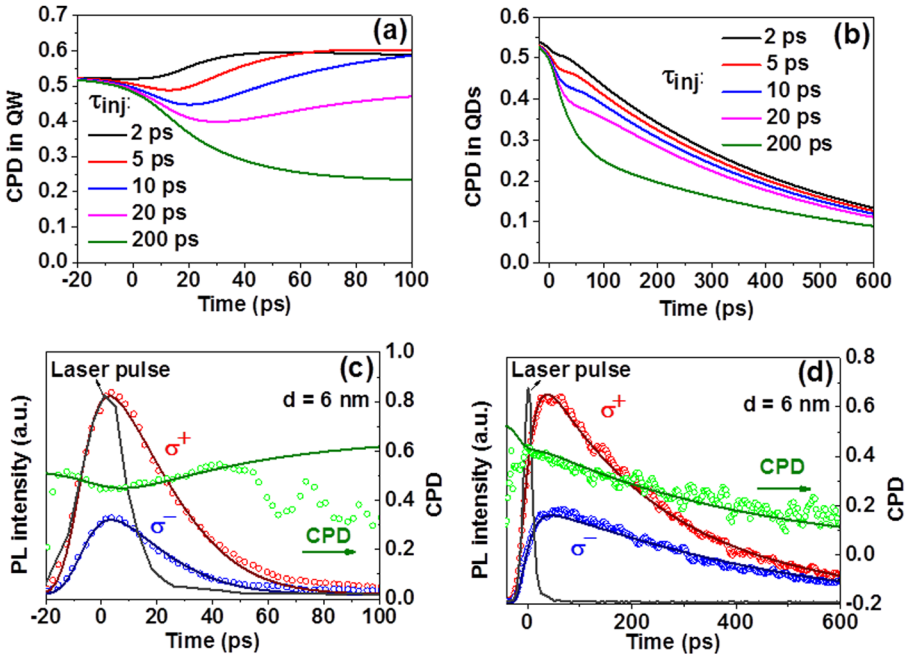


FIG. 2. Rate-equation calculations for time-resolved CPD with various spin-injection times for the (a) QW-PL and (b) QD-PL. $\sigma^+$- (red circles) and $\sigma^-$- (blue circles) polarized TRPL at 20 K, and the CPD (green circles), fitted by the rate-equation calculations (solid lines), in the (c) QW and (d) QDs with $d = 6$ nm, respectively.

The two terms of $\left(1-\frac{N^{\sigma\pm}_{QW}}{D^{\sigma\pm}_{QW}}\right)$ and $\left(1-\frac{N^{\sigma\pm}_{QD-ES}}{D^{\sigma\pm}_{QD-ES}}\right)$ indicate a state filling effect[23] on the limited distribution at the spin-polarized exciton levels in the QW and QDs, where the $D^{\sigma\pm}_{QW}$ and $D^{\sigma\pm}_{QD-ES}$ represent the spin-polarized density of the states at GS in the QW and ES in QDs, respectively. This state filling in the QD is caused by Pauli blocking for the spin-polarized discrete levels due to quantum confinement. Furthermore, we find that the same factor needs to be included in the QW because of localization originating from potential fluctuations due to the alloying and interface mixing between In and Ga atoms. The radiative and non-radiative decay times in the QW and QD are denoted by $\tau^{r}_{QW,\ QD-ES}$ and $\tau^{nr}_{QW,\ QD-ES}$, and $\tau^{sr}_{QW,\ QD-ES}$ are the spin-relaxation times in the QW and QD. These time constants were experimentally deduced from the TRPL of sister samples, such as a single QW and QDs solely prepared under the same growth conditions.

The rate-equation simulations for the time-resolved CPD as a function of $\tau_{inj}$ in the QW and QD, combined with the convolution calculations for the time response of the measurement system, are shown in Figs. 2(a) and 2(b). As we can see, the time-dependence of CPD is still sensitive to the short spin-injection time less than 20 ps. Therefore, we can determine such short injection times from the data fitting. Moreover, faster spin injection is highly beneficial for spin injection into the QD, while slower injection results in rapid decreases in the CPD for both the QW and QDs. These degradations of the spin polarization with longer $\tau_{inj}$ are explained by both the spin relaxation and the state-filling effect.[24] When the injection time is long, the spin state in the QW relaxes prior to the injection. In addition to this, the majority spin state can be occupied immediately after the pulsed excitation and the minority spins only increase if the filling is significant, which results in the decrease of the total spin

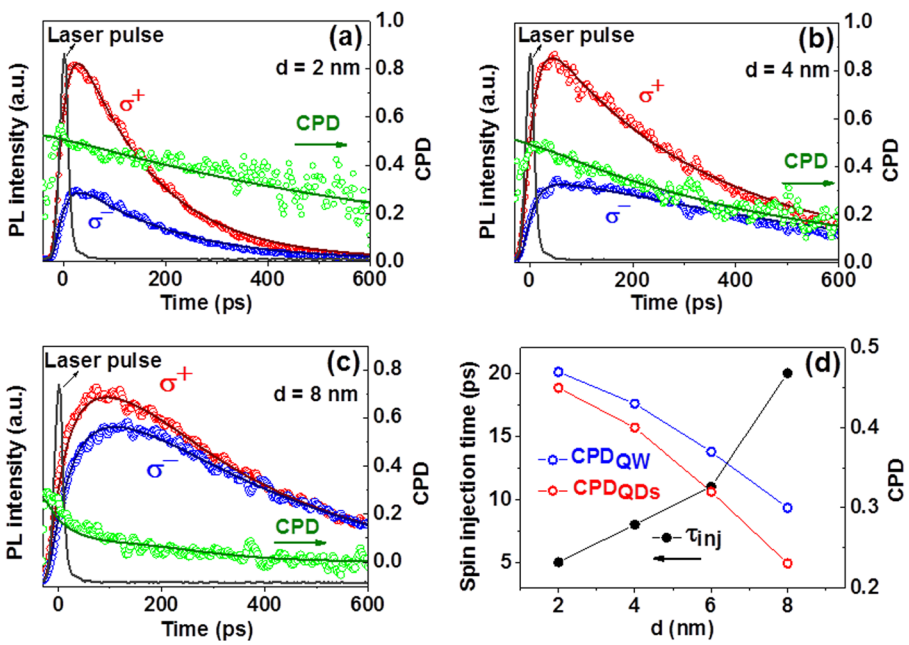


FIG. 3. $\sigma^+$- (red circles) and $\sigma^-$- (blue circles) polarized TRPL, and the CPD (green circles), fitted by the rate-equation calculations (solid lines) in the QDs with (a) $d = 2$ nm, (b) $d = 4$ nm, and (c) $d = 8$ nm, respectively. (d) The barrier-thickness, $d$, dependences of the spin-injection time (filled black circles) and PL-CPDs (open circles).

polarization. According to rate-equation fittings for the TRPL decay profiles in the sample with $d = 6$ nm, shown in Figs. 2(c) and 2(d), $\tau_{inj}$ is deduced to be 11 ps, demonstrating efficient spin injection with the CPD of 0.32 in the QDs. Moreover, we can reasonably fit the experimental data with $\eta^+ \geq 0.94$, and therefore, we conclude that the exciton-spin states are conserved at least 88% during the spin injection into the ES in the QDs. The significant CPD decrease in the previous QW, with $d = 20$ nm in Fig. 1(d), is caused by the strong filling effect because of the strong suppression of tunneling with a sufficiently thick barrier. On the other hand, for thinner barriers with $d \leq 8$ nm, ultrafast tunneling of the spin-polarized excitons relieves the filling effect in the QW, and therefore sustains the conservation of the spin state in the QDs after the injection.

A fast rise of the $\sigma^+$-polarized TRPL and high CPDs from the sample with $d = 2$ nm and $d = 4$ nm, as shown in Figs. 3(a) and 3(b), demonstrate faster and more efficient spin injection. This ultrafast spin injection is elongated in the case of $d = 8$ nm, as shown in Fig. 3(c), originating from slower tunneling through the thicker barrier and resulting in lower CPDs in the QD PL. The barrier-thickness dependences of the spin-injection time and the CPDs in both the QW and QDs are displayed in Fig. 3(d). With decreasing barrier thickness from 8 to 2 nm, the injection time decreases from 20 to 5 ps. Meanwhile, the PL-CPD in the QW increases from 0.30 to 0.47, and the CPD in the QDs shows a similar change from 0.23 to 0.45. As we discussed above, the CPD in the PL can be affected by the filling effect depending on the injection time. The barrier-thickness dependence of $\tau_{inj}$ can be attributed to the tunneling probability as a function of the barrier thickness, where the energy separation and the energy relaxation time after the tunneling inside the QD are identical among these samples with various barrier thicknesses. The shorter spin-injection time can be explained by the stronger coupling of the spin-polarized electron through the thinner GaAs barrier, which is quantitatively confirmed by the wavefunction calculations.

In summary, the coupled InGaAs QW-QDs nanostructures demonstrate ultrafast (5–20 ps) and highly spin-conserved electron-spin injection into the QDs, and strong barrier-thickness dependence. Electronic coupling between QW and QDs enhances the spin transfer and conservation, and implies the promising application in highly efficient spintronic devices.

The authors acknowledge the financial support of the Japan Society for the Promotion of Science (JSPS), Grant-in-Aid for Scientific Research (S) No. 22221007.

[1]A. V. Khaetskii and Y. V. Nazarov, Phys. Rev. B **61**, 12639 (2000).
[2]M. Paillard, X. Marie, P. Renucci, T. Amand, A. Jbeli, and J. M. Gérard, Phys. Rev. Lett. **86**, 1634 (2001).
[3]B. D. Gerardot, D. Brunner, P. A. Dalgarno, P. Öhberg, S. Seidl, M. Kroner, K. Karrai, N. G. Stoltz, P. M. Pertroff, and R. J. Warburton, Nature **451**, 441 (2008).
[4]M. Atatüre, J. Dreiser, A. Badolato, A. Högele, K. Karrai, and A. Imamoglu, Science **312**, 551 (2006).
[5]J. Beyer, I. A. Buyanova, S. Suraprapapich, C. W. Tu, and W. M. Chen, Appl. Phys. Lett. **98**, 203110 (2011).
[6]J. Beyer, I. A. Buyanova, S. Suraprapapich, C. W. Tu, and W. M. Chen, Nanotechnology **23**, 135705 (2012).
[7]R. J. Warburton, Nature Mater. **12**, 483 (2013).
[8]C. H. Li, G. Kioseoglou, O. M. J. van't Erve, M. E. Ware, D. Gammon, R. M. Stroud, B. T. Jonker, R. Mallory, M. Yasar, and A. Petrou, Appl. Phys. Lett. **86**, 132503 (2005).
[9]M. Holub and P. Bhattacharya, J. Phys. D: Appl. Phys. **40**, R179 (2007).
[10]D. Basu, D. Saha, C. C. Wu, M. Holub, Z. Mi, and P. Bhattacharya, Appl. Phys. Lett. **92**, 091119 (2008).
[11]H. Soldat, M. Li, N. C. Gerhardt, M. R. Hofmann, A. Ludwig, A. Ebbing, D. Reuter, A. D. Wieck, F. Stromberg, W. Keune, and H. Wende, Appl. Phy. Lett. **99**, 051102 (2011).
[12]H. Hoüpfner, C. Fritsche, A. Ludwig, A. Ludwig, F. Stromberg, H. Wende, W. Keune, D. Reuter, A. D. Wieck, N. C. Gerhardt, and M. R. Hofmann, Appl. Phys. Lett. **101**, 112402 (2012).
[13]A. Murayama, T. Asahina, K. Nishibayashi, I. Souma, and Y. Oka, Appl. Phys. Lett. **88**, 023114 (2006).
[14]A. Murayama, T. Furuta, K. Hyomi, I. Souma, Y. Oka, D. Dagnelund, I. A. Buyanova, and W. M. Chen, Phys. Rev. B **75**, 195308 (2007).
[15]D. Dagnelund, I. A. Buyanova, W. M. Chen, A. Murayama, T. Furuta, K. Hyomi, I. Souma, and Y. Oka, Phys. Rev. B **77**, 035437 (2008).
[16]Y. I. Mazur, B. L. Liang, Z. M. Wang, D. Guzun, G. J. Salamo, Z. Y. Zhuchenko, and G. G. Tarasov, Appl. Phys. Lett. **89**, 151914 (2006).
[17]V. G. Talalaev, J. W. Tomm, N. D. Zakharov, P. Werner, U. Goüsele, B. V. Novikov, A. S. Sokolov, Y. B. Samsonenko, V. A. Egorov, and G. E. Cirlin, Appl. Phys. Lett. **93**, 031105 (2008).
[18]Y. I. Mazur, V. G. Dorogan, D. Guzun, E. Marega, G. J. Salamo, G. G. Tarasov, A. O. Govorov, P. Vasa, and C. Lienau, Phys. Rev. B **82**, 155413 (2010).
[19]M. Syperek, P. Leszczyński, J. Misiewicz, E. M. Pavelescu, C. Gilfert, and J. P. Reithmaier, Appl. Phys. Lett. **96**, 011901 (2010).
[20]D. Guzun, Y. I. Mazur, V. G. Dorogan, M. E. Ware, E. Marega, G. G. Tarasov, C. Lienau, and G. J. Salamo, J. Appl. Phys. **113**, 154304 (2013).
[21]B. Ohnesorge, M. Albrecht, J. Oshinowo, A. Forchel, and Y. Arakawa, Phys. Rev. B **54**, 11532 (1996).
[22]R. Heitz, H. Born, A. Hoffmann, D. Bimberg, I. Mukhametzhanov, and A. Madhukar, Appl. Phys. Lett. **77**, 3746 (2000).
[23]S. Grosse, J. H. H. Sandmann, G. von Plessen, J. Feldmann, H. Lipsanpen, M. Sopanen, J. Tulkki, and J. Ahopelto, Phys. Rev. B **55**, 4473 (1997).
[24]T. Kiba, X. J. Yang, T. Yamamura, Y. Kuno, A. Subagyo, K. Sueoka, and A. Murayama, Appl. Phy. Lett. **103**, 082405 (2013).